

RESEARCH

Open Access



Elevated *NRAS* expression during DCIS is a potential driver for progression to basal-like properties and local invasiveness

Ze-Yi Zheng^{1,2†}, Hanan Elsarraj^{3†}, Jonathan T. Lei¹, Yan Hong³, Meenakshi Anurag¹, Long Feng^{1,4}, Hilda Kennedy¹, Yichao Shen¹, Flora Lo¹, Zifan Zhao^{1,5}, Bing Zhang¹, Xiang H.-F. Zhang^{1,6}, Ossama W. Tawfik⁷, Fariba Behbod^{3*†} and Eric C. Chang^{1,6*†}

Abstract

Background: Ductal carcinoma in situ (DCIS) is the most common type of in situ premalignant breast cancers. What drives DCIS to invasive breast cancer is unclear. Basal-like invasive breast cancers are aggressive. We have previously shown that *NRAS* is highly expressed selectively in basal-like subtypes of invasive breast cancers and can promote their growth and progression. In this study, we investigated whether *NRAS* expression at the DCIS stage can control transition from luminal DCIS to basal-like invasive breast cancers.

Methods: Wilcoxon rank-sum test was performed to assess expression of *NRAS* in DCIS compared to invasive breast tumors in patients. *NRAS* mRNA levels were also determined by fluorescence in situ hybridization in patient tumor microarrays (TMAs) with concurrent normal, DCIS, and invasive breast cancer, and association of *NRAS* mRNA levels with DCIS and invasive breast cancer was assessed by paired Wilcoxon signed-rank test. Pearson's correlation was calculated between *NRAS* mRNA levels and basal biomarkers in the TMAs, as well as in patient datasets. RNA-seq data were generated in cell lines, and unsupervised hierarchical clustering was performed after combining with RNA-seq data from a previously published patient cohort.

Results: Invasive breast cancers showed higher *NRAS* mRNA levels compared to DCIS samples. These *NRAS*^{high} lesions were also enriched with basal-like features, such as basal gene expression signatures, lower ER, and higher p53 protein and Ki67 levels. We have shown previously that *NRAS* drives aggressive features in DCIS-like and basal-like SUM102PT cells. Here, we found that *NRAS*-silencing induced a shift to a luminal gene expression pattern. Conversely, *NRAS* overexpression in the luminal DCIS SUM225 cells induced a basal-like gene expression pattern, as well as an epithelial-to-mesenchymal transition signature. Furthermore, these cells formed disorganized mammospheres containing cell masses with an apparent reduction in adhesion.

[†]Ze-Yi Zheng and Hanan Elsarraj have contributed equally as co-first authors

[†]Fariba Behbod and Eric C. Chang have contributed equally as co-corresponding authors

*Correspondence: fbehbod@kumc.edu; echang1@bcm.edu

¹ Lester and Sue Smith Breast Center and Dan L. Duncan Comprehensive Cancer Center, Baylor College of Medicine, Houston, TX 77030, USA

³ Department of Pathology and Laboratory Medicine, University of Kansas Medical Center, Kansas City, KS 66160, USA

Full list of author information is available at the end of the article



Conclusions: These data suggest that elevated NRAS levels in DCIS are not only a marker but can also control the emergence of basal-like features leading to more aggressive tumor activity, thus supporting the therapeutic hypothesis that targeting NRAS and/or downstream pathways may block disease progression for a subset of DCIS patients with high NRAS.

Keywords: Breast cancer, DCIS, Premalignancy, Invasion, Ras GTPase

Background

Ductal carcinoma in situ (DCIS) is the most common form of noninvasive breast cancers. In DCIS, cancer cells have expanded inside the breast ducts; however, they have not yet broken through the basement membrane and the myoepithelium to become invasive. The current standard of care for DCIS includes surgery by mastectomy or lumpectomy plus radiation, and endocrine therapy (for hormone receptor-positive DCIS). Although additional radiotherapy and endocrine therapy have resulted in significant improvement in prevention of invasive breast cancer recurrence, they have not resulted in improved patient survival. Thus, the 20-year breast cancer mortality rate following a DCIS diagnosis, with or without additional radiation and endocrine therapy, remains at 3.3% [1].

Studies that have investigated the natural progression of human DCIS have reported untreated DCIS to progress to invasive breast cancer at a rate of approximately 40% [2]. Untreated DCIS are those that were originally misdiagnosed with benign breast diseases but had subsequent examination with DCIS or those with biopsy proven DCIS who underwent non-operative management [3–5]. The risk factors significantly associated with the development of invasive disease are high grade, calcifications, younger age (<60 years), absence of endocrine therapy, and lesion size [2, 6]. Currently, two diagnostic tests have been developed for risk stratification in DCIS, DCIS Score™, and DCISionRT [7–9]. These tools have not yet been widely adopted, and their clinical utility remains unclear.

Basal-like breast cancers account for 10–20% of all invasive breast cancers, and they are highly proliferative and very aggressive [10]. These tumors are called “basal-like” because they express markers of the basal region in the mammary structure. These basal-like tumors are usually, but not always, triple-negative for ER, PR, and HER2. Interestingly, premalignant lesions prior to DCIS (such as atypical ductal hyperplasia, ADH) are nearly all ER⁺, and basal-like lesions first appear at DCIS at a frequency of 4–8% [11]. Furthermore, it has been noted for some time that patients whose tumors are initially ER⁺ can later become ER⁻ when they relapse after endocrine therapy [12]. These data suggest that luminal breast tumor cells have a

great degree of plasticity, and that they can evolve into cancer cells with basal-like properties during DCIS progression, which may lead to the emergence of invasive breast cancers.

The Ras superfamily of GTPases are encoded by three RAS genes, HRAS, NRAS, and KRAS. Oncogenic RAS mutations, which lock the RAS proteins in the GTP-bound state, can be found in approximately 30% of human cancers [13]; however, RAS oncogenic mutations are very rare in primary breast cancer [14]. Instead, we have shown previously that *wild-type* NRAS is selectively overexpressed in the basal-like breast cancers [15]. By gene silencing, NRAS has been demonstrated to be necessary for the growth of basal-like breast cancer cells but not that of luminal breast cancer cells or the closely related claudin-low cells [15]. More importantly, we have evidence that NRAS overexpression can promote more aggressive tumor activity, such as tumor formation in mice when co-transplanted with fibroblasts [15]. In support of these findings, a more recent clinical study of 198 previously untreated breast cancer patients with long-term follow-up showed that among the RAS family members, NRAS expression was significantly associated with triple negativity, higher grade, and reduced overall and disease-free survival. In the multivariable analysis, elevated NRAS mRNA independently predicted reduced overall and disease-free survival [16].

In this study, we investigated whether NRAS is responsible for the emergence of basal-like properties during DCIS and invasiveness. Our results suggest that N-Ras is not only a biomarker for invasiveness that it can also drive the emergence of basal-like properties from luminal cells.

Methods

Cell culture media and general reagents

SUM102PT and SUM102PT cells carrying DOX-inducible shRNA against NRAS were as described previously [15]. SUM225 cells were cultured in DMEM/F12 medium (Thermo Fisher Scientific) supplemented with 5% fetal bovine serum (Sigma-Aldrich), 10 mM HEPES (Thermo Fisher Scientific), non-essential amino acids (Thermo Fisher Scientific), 5 µg/mL human insulin (Sigma-Aldrich), and 1 µg/mL hydrocortisone (Sigma-Aldrich).

Mammosphere formation assay

DOX-inducible *N-RAS* overexpressed SUM225 cells used in mammosphere experiment were created by transiently infect the cells with lentivirus carrying pINDUCER-NRAS as previously described [15]. Single cells were plated on ultra-low attachment 24-well plates (Corning) at a density of 5,000 viable cells per well. Cells were grown in serum-free mammary epithelial basal medium (Lonza) supplemented with 20 ng/ml EGF, 5 µg/ml insulin, 1 µg/ml hydrocortisone (Lonza), 20 ng/ml β-FGF, B27 (Invitrogen), 4 µg/ml heparin (MP Biomedicals), and Antibiotic–Antimycotic (Invitrogen). Cells were fed every three days by adding an additional media (10% of total volume) to the wells. When noted, 2 µg/ml DOX was also added. Mammospheres were cultured for 1.5 or 3 months before being examined and photographed on an Olympus IX71 microscope. The numbers of abnormal vs normal spheres were counted in a double-blind fashion.

Detection of *NRAS* expression in TMAs by FISH

TMAs were constructed from paraffin-embedded, formalin-fixed (FFPE) sections of breast tissue from patients diagnosed with concurrent DCIS and IDC ($n=22$). The samples in the TMAs were obtained from individuals enrolled under an IRB-approved protocol and following US Common Rule.

FISH procedures were performed using RNAscope[®] Probe-Hs-*NRAS* (Advanced Cell Diagnostics), RNAscope[®] Negative Control Probe-DapB (Advanced Cell Diagnostics), and RNAscope Multiplex Fluorescent Reagent Kit V2 (Advanced Cell Diagnostics) on FFPE sections, according to manufacturer's instructions. Data analysis was performed using ImageJ. Each fluorophore channel was analyzed separately. The region of interest (ROI) was selected around the DCIS or invasive lesions. A number of cells in ROI were quantified by counting Hoechst positive nuclei (number of nuclei/ROI). FISH signals were then analyzed in the same ROI (number of signals/ROI). The “average number of signal/cell” was calculated by dividing “number of signals/ROI” by “number of nuclei/ROI.” At least three images per patient were analyzed.

qPCR

RNA was isolated using RNeasy kit (Qiagen), and cDNAs were synthesized using SuperScript IV First-Strand Synthesis System (Thermo Fisher Scientific). Real-time PCR was conducted with Power SYBR Green Master Mix (Thermo Fisher Scientific) on a CFX Real-Time PCR system (Bio-Rad). The primers (5' → 3') used were: *NRAS*, forward: TGGTGGTTGGAGCAGGTG; reverse: GCC TTCGCTGTCCTCATGTA. *KRT8*, forward: AGCGTA

CAGAGATGGAGAACGA; reverse: AGCTCCCGG ATCTCCTCTTC. *ACTB*, forward: CACCATTGGCAA TGAGCGGTTC; reverse: AGGTCTTTGCGGATGTCC ACGT. The relative amounts of PCR products generated from each primer set were determined on the basis of threshold cycle (Ct) using *ACTB* as the loading control.

RNA-seq

SUM102PT carrying DOX-inducible shRNA against *NRAS* [15] was seeded with or without 2 µg/ml DOX for 3 months. To maintain *NRAS* silencing, fresh DOX was added when the medium was replenished. To overexpress *NRAS*, pBABE-*NRAS* [15] or pBABE vector control was used to transduce SUM225 cells, which were then selected in 1 µg/ml puromycin for 2 days. The resulting cells were grown in puromycin-free medium for five weeks. One µg of total RNA isolated by RNeasy Mini Kit (QIAGEN) was sent to Novogene for RNA quality control (Agilent 2100 Bioanalyzer), library preparation, and next-generation sequencing (Illumina NovaSeq 6000). For RNA-seq processing, paired-end 150 bp reads were aligned to hg19 (GRCh37) reference genome using RSEM v1.2.31 [17] and Bowtie 2 [18]. Log2 RSEM counts of protein-coding genes were upper quantile normalized and used for downstream analysis. The RNA-seq data have been submitted to the GEO public database (GSE215407).

Breast cancer patient transcriptomic profiling datasets

Two published breast cancer microarray datasets (GSE59248 and GSE26304) were used for *NRAS* expression analysis. They were downloaded from NCBI Gene Expression Omnibus (<https://www.ncbi.nlm.nih.gov/geo/>) as matrix files in txt format. In GSE59248, microarray was performed on Agilent-028004 SurePrint G3 Human GE 8 × 60 K Microarray Platform (GPL13607) and mean values of all probes mapping to a gene were taken for downstream analysis. In GSE26304, microarray was performed on Agilent-012391 Whole Human Genome Oligo Microarray G4112A (GPL6848), and there was one probe for *NRAS* without replicates. In addition, RNA-seq from a CPTAC breast cancer study was used [19].

Statistical analysis

Pearson correlation coefficients in Table 1 were calculated between *NRAS* mRNA expression levels for each breast biomarker (ER, PR, HER2, Ki67, and P53) by correlating the average *NRAS* mRNA signal per cell and biomarker expression in each DCIS and IDC patient.

All RNA-seq statistical analysis was performed in R (version 4.0.2). The R package limma [20] was used to compute differences by moderated t-test for each gene. Signed $-\log_{10}$ p values from limma analyses were used

Table 1 Up-regulation of *NRAS* expression levels correlates with features found commonly in basal-like tumors

	<i>NRAS</i> versus ER ¹ , <i>n</i> = 21		<i>NRAS</i> versus PR, <i>n</i> = 21		<i>NRAS</i> versus HER2, <i>n</i> = 16		<i>NRAS</i> versus Ki67, <i>n</i> = 20		<i>NRAS</i> versus p53, <i>n</i> = 17	
	DCIS	IDC	DCIS	IDC	DCIS	IDC	DCIS	IDC	DCIS	IDC
Pearson Correlation:	-0.49	-0.52	-0.31	0.09	0.24	0.3	0.55	0.68	0.54	0.55
<i>P</i> (two-tailed):	0.0341	0.0148	0.2133	0.7012	0.3991	0.2563	0.0187	0.0009	0.0364	0.0233

¹ ER, HER2, Ki67, and p53 levels were measured by IHC. *NRAS* levels were assessed by FISH. See Additional file 1: Table S1 for the levels of biomarkers

as input for Gene Set Enrichment Analysis using default parameters with WebGestalt [21]. Specific methods used to calculate *p* values are also described in each figure legend. To combine RNA-seq data from breast tumors in the CPTAC cohort [19], RSEM-normalized log₂-transformed counts were combined with cell line data generated in this study. The entire dataset was then batch corrected with ComBat-seq [21] before clustering using the top 1,000 genes with highest variance across the combined dataset with ComplexHeatmap [22] with the following parameters: clustering_distance_columns = “spearman,” clustering_distance_rows = “euclidean,” clustering_method_rows = “ward.D2.”

Results

High *NRAS* expression levels in DCIS samples from patients correlate with invasion

To assess whether N-Ras can control progression during DCIS, we first examined a microarray data set derived from a study comparing gene expression levels in DCIS vs. invasive breast cancer [23]. Our analysis revealed that *NRAS* mRNA levels were significantly higher in invasive breast tumors than in DCIS (Fig. 1A).

Next, we took an orthogonal approach to study the relationship between *NRAS* mRNA levels and DCIS progression. *NRAS*-specific antibodies are not available for robust analyses of clinical samples [24], and we thus performed fluorescence in situ hybridization (FISH) on tissue microarrays (TMAs) consisting of 22 concurrent DCIS/IDC lesions, as well as adjacent normal tissues (Additional file 1: Table S1). Using an *NRAS*-specific probe (Fig. 1B), the FISH data were quantified to show that *NRAS* mRNA levels are significantly higher in DCIS than in the normal regions (Fig. 1C, E). Moreover, *NRAS* levels are higher in IDC than in DCIS regions (Fig. 1C, E), suggesting a progressive increase of expression from normal, DCIS, to IDC.

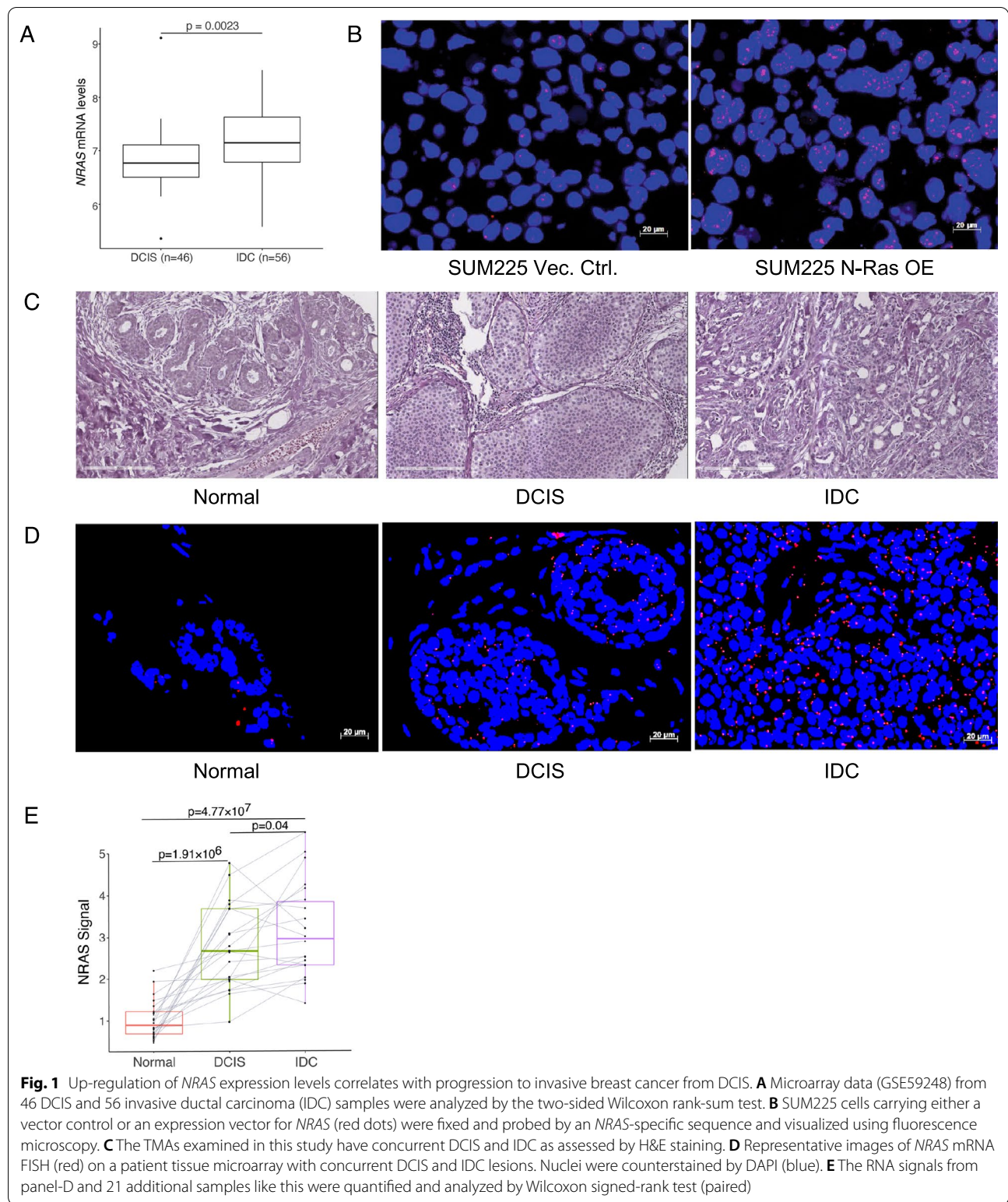
NRAS expression correlated with basal-like features in DCIS patient samples

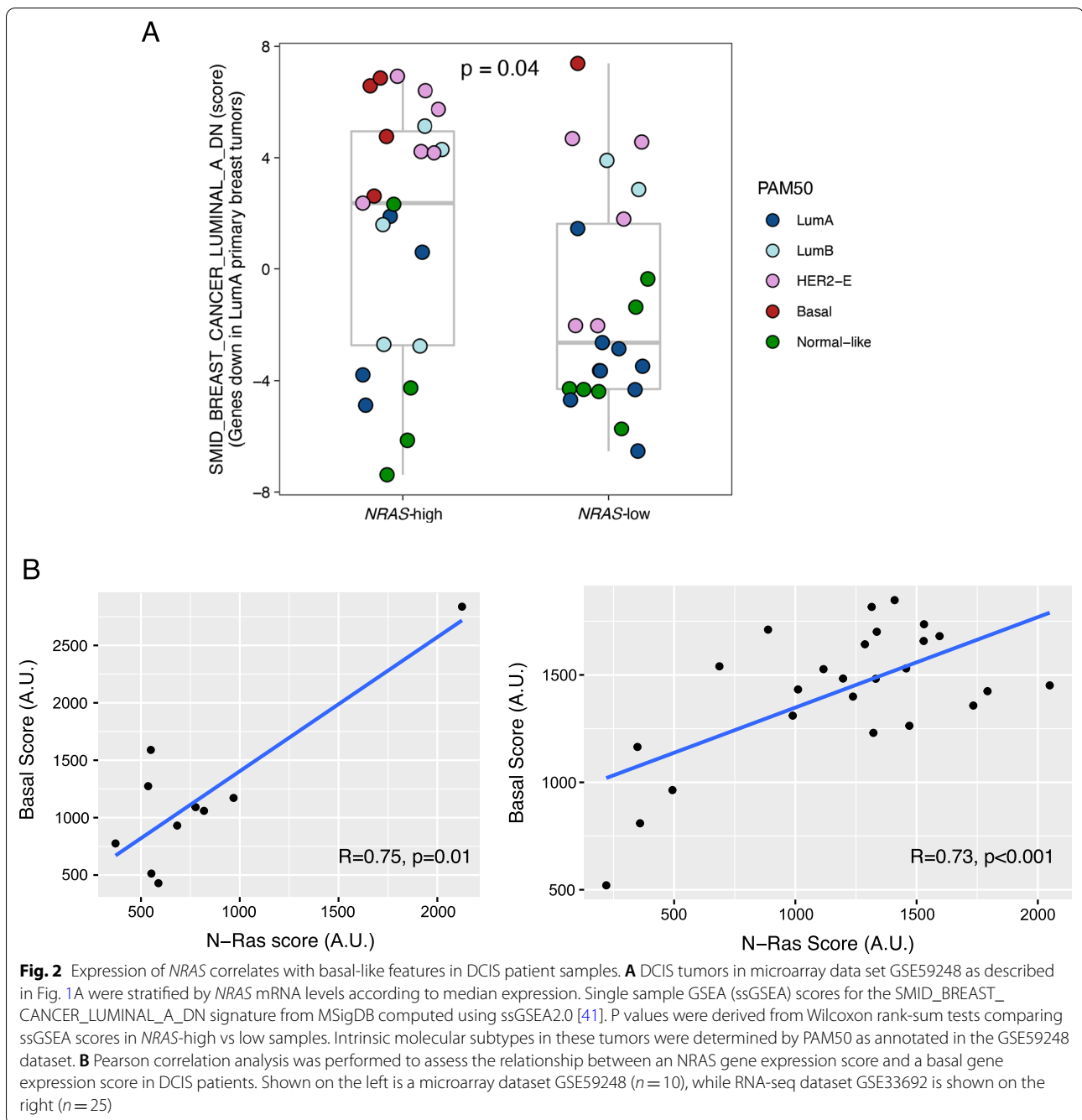
To investigate the role of *NRAS* in the emergence of basal-like properties during DCIS, we first analyzed the same microarray dataset as described in Fig. 1A to

determine whether *NRAS* mRNA levels were associated with basal-like properties. We examined a dataset [25] for a gene signature that is down-regulated in primary luminal-A tumors, as compared to basal tumors. The data show that this luminal-A down-regulated gene signature is expressed at significantly higher levels in DCIS samples with high *NRAS* levels (Fig. 2A). We note that the great majority of DCIS tumors displayed basal properties, as determined by PAM50 [26], also have higher levels of *NRAS* mRNA (see below for more analysis).

We have previously uncovered a gene signature associated with *NRAS* expression in basal-like breast cancer [15]. As shown in Fig. 2B, we applied this signature as an orthogonal approach to assess the role of *NRAS* signaling in two additional DCIS cohorts [27, 28] and found a significant correlation with this basal-like gene signature [29].

Finally, we further investigated the relationship between *NRAS* expression levels and basal-like properties in the aforementioned TMA sample set. These patient concurrent DCIS/IDC samples were evaluated for the expression of clinically relevant biomarkers including ER, PR, HER2, Ki67 and P53 (Additional file 1: Table S1). A correlation between the expression of these biomarkers and *NRAS* expression was performed using Pearson correlation. These studies showed that among the evaluated biomarkers, *NRAS* expression showed a significant correlation with basal-like features: low ER and high Ki67 (Table 1). Furthermore, basal-like tumors frequently carry *TP53* mutations [30]. Wild-type p53 has a very short half-life; thus, it is usually undetectable by IHC; however, mutant p53 protein levels can be more readily detected by IHC [31]. We observed higher p53 levels in *NRAS*^{high} tumors (Table 1), agreeing with the concept that these tumors display basal properties. These included both the DCIS and IDC regions of concurrent DCIS/IDC samples. Collectively, these clinical data support the concept that *NRAS* plays a key role in the emergence of basal-like high proliferative features during DCIS-IDC transition.





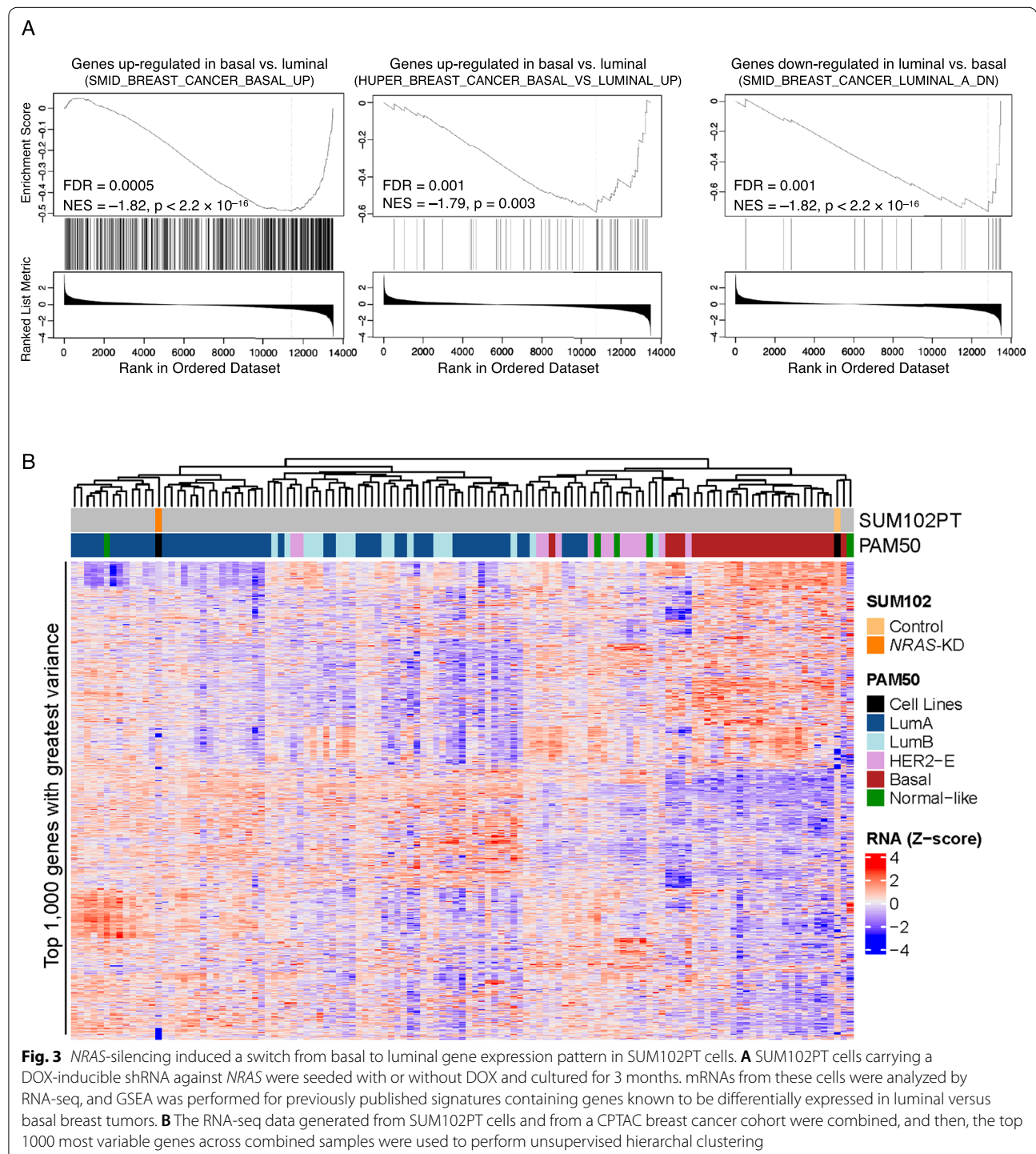
***NRAS*-silencing in basal DCIS-like cells induces a luminal gene expression pattern**

The clinical data demonstrated a strong correlation between up-regulation of *NRAS* in the mostly luminal DCIS and the emergence of basal-like properties and more aggressive tumor activities, such as higher level of proliferation and invasion. To ascertain whether *NRAS* plays a more direct role in controlling the balance between luminal to basal properties during DCIS,

we turned to a basal-like and DCIS-like cell line model, SUM102PT [32]. We have shown previously that this cell line has high levels of *NRAS* (as compared to cell lines of other breast cancer subtypes) and *NRAS* can promote tumor growth of these cells in vivo [15]. In this study, we knocked down (KD) *NRAS* expression using a DOX-inducible shRNA clone as reported previously [15], and mRNAs were harvested over a four-month period. DOX was replenished when medium was changed to

maintained *NRAS* silencing (Additional file 2: Fig. S1). To select the appropriate time points for RNA-seq, we performed qPCR to measure the expression of a luminal marker, *CK8/KRT8* (Additional file 2: Fig. S1). We thus generated RNA-seq data on these SUM102PT cells after three months in the presence of DOX (Additional

file 3: Table S2) and performed Gene Set Enrichment Analysis (GSEA) to analyze datasets derived from examining differential gene expression between luminal and basal breast cancer cells (Additional file 3: Table S2). We found that genes that are down-regulated in *NRAS*^{KD} SUM102PT cells matched genes that are known to be



up-regulated in basal breast cancer cells in at least two datasets [25, 33] (Fig. 3A). Consistent with the possibility that these genes are enriched in basal-like cells, they were down-regulated in luminal breast cancer cells as seen in a previous study [25] (Fig. 3A). These results support the hypothesis that *NRAS*-silencing reduced expression of genes typically up-regulated in basal-like breast cancer cells.

Next, the SUM102PT RNA-seq data were combined with RNA-seq data from a recent Clinical Proteomic Tumor Analysis Consortium (CPTAC) breast cancer cohort study [19]. Top 1,000 most variable genes (Additional file 3: Table S2) were used to perform unsupervised hierarchical clustering. Our data showed that while the *NRAS*⁺ SUM102PT control cells clustered together with tumors of the basal-like subtype as expected, the *NRAS*-silenced set from these cells clustered with the luminal-A subtype (Fig. 3B).

***NRAS* overexpression in luminal DCIS cells induces basal-like features**

We performed the converse experiment by stably overexpressing *NRAS* [15] in a luminal DCIS model cell line SUM225 (Fig. 1B). RNA-seq data (Additional file 4: Table S3) revealed that the gene expression patterns in the N-Ras overexpressing SUM225 cells were mostly clustered with those from the basal-like tumors in the same CPTAC patient cohort as described above (Fig. 4A). In contrast, SUM225 cells carrying the vector control displayed a mostly luminal-like gene expression pattern as expected.

To further analyze what biological activities were perturbed by *NRAS* expression, we performed GSEA (Additional file 4: Table S3, Fig. 4B). The data showed that the top hallmark pathways induced after *NRAS* overexpression are enriched with immune/inflammatory pathways, which is similar to what has been reported previously in basal-like breast tumors [15]. These results agree with the concept that *NRAS* overexpression can promote a shift from luminal to basal-like properties. Furthermore, an epithelial to mesenchymal transition (EMT) signature was among the pathways significantly correlated with *NRAS* expression (Fig. 4B). This is a feature that is

usually observed in cells with more invasive potentials, but future validation is needed.

We also seeded *NRAS*-overexpressing SUM225 cells for mammosphere formation, in which the number and size of the sphere are typically assessed for stem-like properties. We did not observe any major difference in the number of spheres with respect to *NRAS* expression status. In the absence of DOX, SUM225 cells mostly form organized mammospheres that are round (Fig. 4C). These mammospheres have low cell density in the middle, which is surrounded by a distinct membrane boundary. In contrast, the *NRAS*-overexpressing SUM225 cells (+DOX) formed disorganized structures in which dense cell masses appear to spread out easily. These subtype-specific mammosphere features agree with those observed using human breast cancer cells and mouse mammary cells [34, 35]. The size of these abnormal spheres is usually larger than the round one regardless of *NRAS* expression status.

Discussion

The molecular mechanisms that drive a transition from DCIS to IDC are currently largely unknown, leading to overtreatment. Our analyses of patient samples illustrate that *NRAS* expression levels in DCIS correlate with invasiveness, as well as with biomarkers associated with high risks for progression such as low ER and high Ki67 [28, 36, 37]. Moreover, *NRAS* mRNA levels and *NRAS* gene expression signature correlate with basal-like properties in DCIS. *NRAS* silencing in a basal-like DCIS cells can induce luminal gene expression patterns; conversely, *NRAS* overexpression promotes basal-like gene signatures in luminal DCIS cells. These results support our conclusion that *NRAS* may be overexpressed by clonal subpopulations within DCIS that drive the emergence of basal invasive breast cancers.

Bergholtz and colleagues [38] analyzed 57 pure DCIS and 313 invasive breast cancer by gene expression, DNA methylation, and DNA copy number. Their studies found that the most significant differences were observed between basal-like DCIS and basal-like IDC. Basal-like DCIS showed lower correlation with core basal-like gene

(See figure on next page.)

Fig. 4 *NRAS* overexpression induces basal-like features in a human luminal DCIS model SUM225. **A** SUM225 cells overexpressing N-Ras and the counterparts carrying the vector control were cultured for 5 weeks. The RNA-seq data generated from these SUM225 cells and from the same CPTAC breast cancer cohort as in Fig. 3B were combined, and then, the top 1000 most variable genes across combined samples were used to perform unsupervised hierarchical clustering. **B** Gene Set Enrichment Analysis on Hallmark gene sets was performed using signed $-\log_{10} p$ values from limma results. Gene sets represented as red bars are up-regulated, while blue bars are down-regulated in *NRAS*-overexpressing SUM225 cells. **C** SUM225 cells carrying a DOX-inducible vector to overexpress *NRAS* were seeded with or without DOX in low attachment dishes for mammosphere formation. Normal spheres that are mostly round with a smooth boundary were counted as normal (top). The disorganized spheres usually have irregular shapes with cell masses that protrude from the boundary. Bar = 200 μm . Whether the portions of disorganized spheres are more common in *NRAS* overexpressing cells (+DOX) in two separate experiments was examined by Fisher's exact test (bottom)

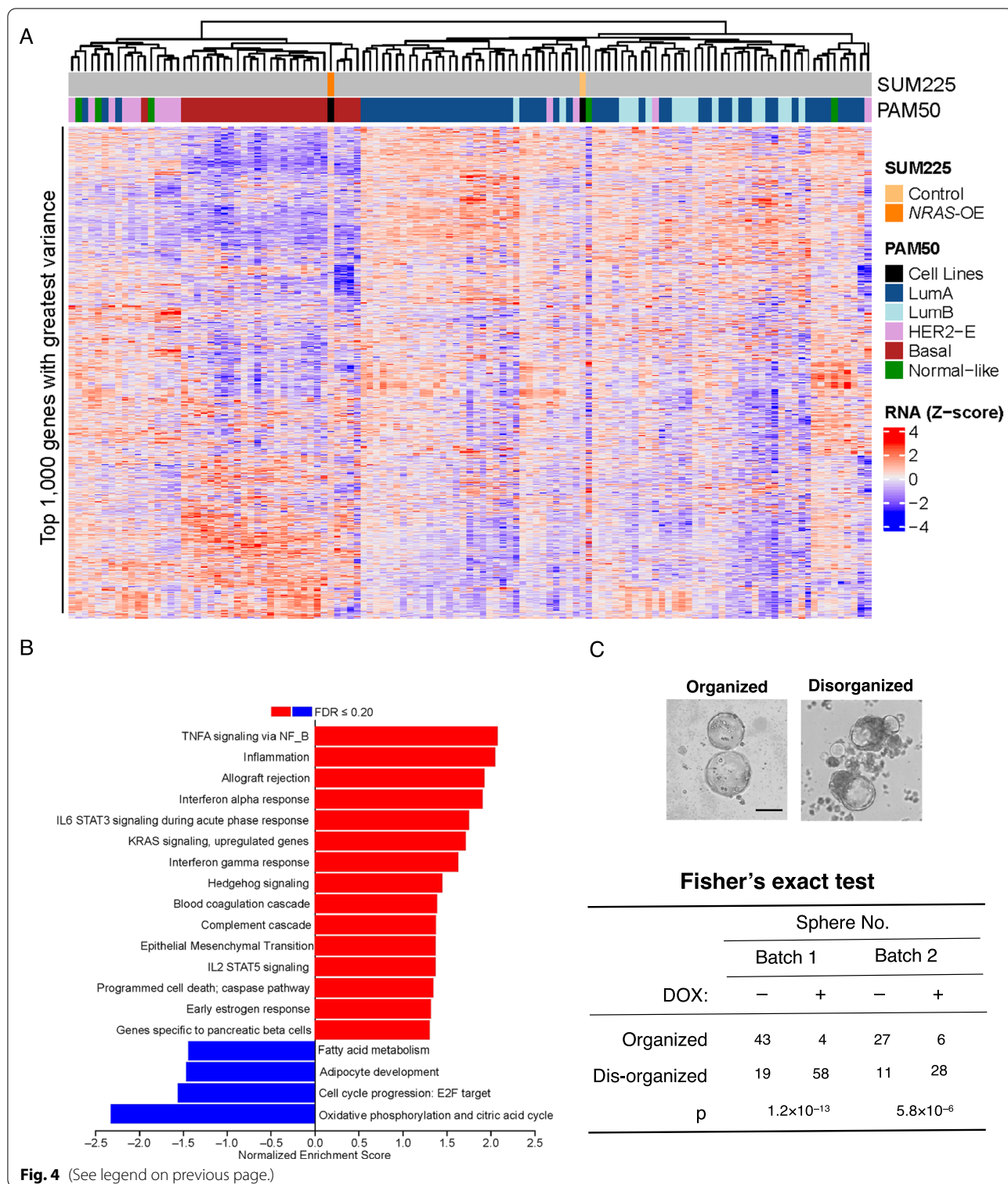


Fig. 4 (See legend on previous page.)

signature, as compared to basal-like IDC. Interestingly, basal-like DCIS showed higher correlation with luminal-A subtype, higher degree of differentiation, and lower proliferation rate. Furthermore, basal DCIS showed

fewer copy number aberrations compared to basal-like IDC. These data suggest that basal-like IDC may evolve from non-basal-like DCIS, such as a subset of luminal DCIS in which *NRAS* is overexpressed.

We have shown that N-Ras itself can be targeted for degradation as a potential therapeutic strategy [39]. Furthermore, N-Ras appears to act via JAK2 to turn on IL8 expression in basal-like breast cancer [15]. Therefore, another potential therapeutic strategy may be to block Jak2 activation and or to use an IL8 blocker at the stage of DCIS. Reparixin is an orally bioavailable inhibitor for IL8 receptors, CXCR1/CXCR2. Reparixin was recently evaluated in a Phase II clinical trials in combination with Paclitaxel for patients with metastatic TNBC [40]. While the primary endpoint of prolonged progression-free survival was not met, the expression of *NRAS* may be a potential biomarker of response in these patients in future studies.

Conclusion

After a DCIS diagnosis, a key problem is whether to treat the patients given the fact that only up to 40% of untreated DCIS cases will progress to invasive disease. Our study is the first to demonstrate *NRAS* as a potential driver of DCIS transition to invasion, and both *NRAS* and its downstream effector are druggable. Despite our promising results with a small sample size, future studies evaluating a larger patient cohort and efficacy studies using *NRAS* targeting agents to inhibit progression to IDC should be pursued.

Abbreviations

CPTAC: Clinical proteomic tumor analysis consortium; DCIS: Ductal carcinoma in situ; DOX: Doxycycline; FFPE: Formalin-fixed paraffin embedded; FISH: Fluorescence in situ hybridization; GSEA: Gene Set Enrichment Analysis; IBC: Invasive breast cancer; IDC: Invasive ductal carcinoma; KD: Knock down; OE: Overexpression; TMA: Tumor microarray; TNBCs: Triple negative breast cancers.

Supplementary Information

The online version contains supplementary material available at <https://doi.org/10.1186/s13058-022-01565-5>.

Additional file 1: Table S1. Pathological, Biomarker and Demographic Characteristics of the patients in the TMAs.

Additional file 2. Figure S1, related to Figure 3 — measuring *NRAS* and *KRT8* expression over time after gene silencing.

Additional file 3: Table S2. *NRAS*-silencing induced a switch from basal to luminal gene expression pattern in SUM102PT cells as measured by RNA-seq.

Additional file 4: Table S3. *NRAS* overexpression induces basal-like features in a human luminal DCIS model SUM225 cells.

Acknowledgements

Not applicable.

Author contributions

ZYZ, FB, and ECC are responsible for the design, analysis, and overall execution of the experiments. ZYZ, HE, JTL, YH, MA, LF, HK, YS, FL, ZZ, BZ, XHZ, and OWT conducted the experiments and/or data analysis. The paper was written mostly by ZYZ, FB, and ECC and reviewed by all authors. All authors read and approved the final manuscript.

Funding

This study was supported by grants from the following agencies: NIH: P50CA186784 (EC), R01CA207445 (FB), P30CA168524 (FB), and R21CA226567 (EC and FB). DoD: W81XWH-21-1-0107, W81XWH-21-1-0106, W81XWH-19-1-0527, and W81XWH-21-1-0634 (EC). Cancer Prevention & Research Institutes of Texas (CPRIT): BZ is a CPRIT Scholar and support by the CPRIT award RR160027. Cancer Research UK and KWF Kankerbestrijding (ref. C38317/A24043) (FB). The Kansas Institute for Precision Medicine – COBRE (P20 GM130423) (FB). NCATS Frontiers-CTSA grant from NCATS awarded to the University of Kansas for Frontiers, ref# UL1TR002366 (FB).

Availability of data and materials

RNA-seq generated by this study for SUM102PT and SUM225 cell lines has been deposited in the GEO public database, and access will be given when the paper is ready for publication. Processed Log2 RSEM upper quantile normalized data needed for analysis are already in Additional file 3: Table S2 and Additional file 4: Table S3.

Declarations

Ethics approval and consent to participate

Patients gave written informed consent for participation in this University of Kansas Medical Center Institutional Review Board approved study, which allowed collection of de-identified surgical tissue for research. The rest of the gene expression patient datasets are already published and publicly available.

Consent for publication

Our study does not contain any individual data, and all authors have approved the contents in this manuscript.

Competing interests

All authors declared no conflict or personal or financial interests, except BZ who received personal fees from AstraZeneca and TNIK PHARMACEUTICALS LTD outside the submitted work.

Author details

¹Lester and Sue Smith Breast Center and Dan L. Duncan Comprehensive Cancer Center, Baylor College of Medicine, Houston, TX 77030, USA. ²Department of Medicine, Baylor College of Medicine, Houston, TX 77030, USA. ³Department of Pathology and Laboratory Medicine, University of Kansas Medical Center, Kansas City, KS 66160, USA. ⁴Department of Pathogenic Organism Biology, Henan University of Chinese Medicine, Zhengzhou, People's Republic of China. ⁵Cancer Cell Biology Graduate Program, Baylor College of Medicine, Houston, TX 77030, USA. ⁶Department of Molecular and Cellular Biology, Baylor College of Medicine, Houston, TX 77030, USA. ⁷MAWD Pathology Group, St. Luke's Hospital, Lenexa, KS 66215, USA.

Received: 7 August 2022 Accepted: 6 October 2022

Published online: 18 October 2022

References

- Narod SA, Iqbal J, Giannakeas V, Sopik V, Sun P. Breast cancer mortality after a diagnosis of ductal carcinoma in situ. *JAMA Oncol.* 2015;1(7):888–96.
- Maxwell AJ, Hilton B, Clements K, Dodwell D, Dulson-Cox J, Kearins O, Kirwan C, Litherland J, Mylvaganam S, Provenzano E, et al. Unresected screen-detected ductal carcinoma in situ: outcomes of 311 women in the forget-me-not 2 study. *Breast.* 2022;61:145–55.
- Collins LC, Tamimi RM, Baer HJ, Connolly JL, Colditz GA, Schnitt SJ. Outcome of patients with ductal carcinoma in situ untreated after diagnostic biopsy: results from the Nurses' Health Study. *Cancer.* 2005;103(9):1778–84.
- Page DL, Dupont WD, Rogers LW, Landenberger M. Intraductal carcinoma of the breast: follow-up after biopsy only. *Cancer.* 1982;49(4):751–8.
- Sanders ME, Schuyler PA, Dupont WD, Page DL. The natural history of low-grade ductal carcinoma in situ of the breast in women treated by biopsy only revealed over 30 years of long-term follow-up. *Cancer.* 2005;103(12):2481–4.

6. Maxwell AJ, Clements K, Hilton B, Dodwell DJ, Evans A, Kearins O, Pinder SE, Thomas J, Wallis MG, Thompson AM, et al. Risk factors for the development of invasive cancer in unresected ductal carcinoma in situ. *Eur J Surg Oncol*. 2018;44(4):429–35.
7. Marshall E. Breast cancer. Dare to do less *Science*. 2014;343(6178):1454–6.
8. Warnberg F, Karlsson P, Holmberg E, Sandelin K, Whitworth PW, Savala J, Barry T, Leesman G, Linke SP, Shivers SC, et al. Prognostic risk assessment and prediction of radiotherapy benefit for women with ductal carcinoma in situ (DCIS) of the breast, in a randomized clinical trial (SweDCIS). *Cancers*. 2021;13(23):6103.
9. Bremer T, Whitworth PW, Patel R, Savala J, Barry T, Lyle S, Leesman G, Linke SP, Jirstrom K, Zhou W, et al. A biological signature for breast ductal carcinoma in situ to predict radiotherapy benefit and assess recurrence risk. *Clin Cancer Res*. 2018;24(23):5895–901.
10. Sorlie T, Perou CM, Tibshirani R, Aas T, Geisler S, Johnsen H, Hastie T, Eisen MB, van de Rijn M, Jeffrey SS, et al. Gene expression patterns of breast carcinomas distinguish tumor subclasses with clinical implications. *Proc Natl Acad Sci U S A*. 2001;98(19):10869–74.
11. Zhou W, Jirstrom K, Amini RM, Fjallskog ML, Sollie T, Lindman H, Sorlie T, Blomqvist C, Warnberg F. Molecular subtypes in ductal carcinoma in situ of the breast and their relation to prognosis: a population-based cohort study. *BMC Cancer*. 2013;13:512.
12. Kuukasjarvi T, Kononen J, Helin H, Holli K, Isola J. Loss of estrogen receptor in recurrent breast cancer is associated with poor response to endocrine therapy. *J Clin Oncol*. 1996;14(9):2584–9.
13. Pylayeva-Gupta Y, Grabocka E, Bar-Sagi D. RAS oncogenes: weaving a tumorigenic web. *Nat Rev Cancer*. 2011;11(11):761–74.
14. Griffith OL, Spies NC, Anurag M, Griffith M, Luo J, Tu D, Yeo B, Kunisaki J, Miller CA, Krysiak K, et al. The prognostic effects of somatic mutations in ER-positive breast cancer. *Nat Commun*. 2018;9(1):3476.
15. Zheng ZY, Tian L, Bu W, Fan C, Gao X, Wang H, Liao YH, Li Y, Lewis MT, Edwards D, et al. Wild-type N-Ras, overexpressed in basal-like breast cancer, promotes tumor formation by inducing IL-8 secretion via JAK2 activation. *Cell Rep*. 2015;12(3):511–24.
16. Banys-Paluchowski M, Milde-Langosch K, Fehm T, Witzel I, Oliveira-Ferrer L, Schmalfeldt B, Muller V. Clinical relevance of H-RAS, K-RAS, and N-RAS mRNA expression in primary breast cancer patients. *Breast Cancer Res Treat*. 2020;179(2):403–14.
17. Li B, Dewey CN. RSEM: accurate transcript quantification from RNA-Seq data with or without a reference genome. *BMC Bioinformatics*. 2011;12:323.
18. Langmead B, Salzberg SL. Fast gapped-read alignment with Bowtie 2. *Nat Methods*. 2012;9(4):357–9.
19. Krug K, Jaehnnig EJ, Satpathy S, Blumenberg L, Karpova A, Anurag M, Miles G, Mertins P, Gefen Y, Tang LC, et al. Proteogenomic landscape of breast cancer tumorigenesis and targeted therapy. *Cell*. 2020;183(5):1436–1456 e1431.
20. Ritchie ME, Phipson B, Wu D, Hu Y, Law CW, Shi W, Smyth GK. limma powers differential expression analyses for RNA-sequencing and microarray studies. *Nucleic Acids Res*. 2015;43(7):e47.
21. Zhang Y, Parmigiani G, Johnson WE. ComBat-seq: batch effect adjustment for RNA-seq count data. *NAR Genom Bioinf*. 2020;2(3):lqaa078.
22. Gu Z, Eils R, Schlesner M. Complex heatmaps reveal patterns and correlations in multidimensional genomic data. *Bioinformatics*. 2016;32(18):2847–9.
23. Lesurf R, Aure MR, Mork HH, Vitelli V, Oslo Breast Cancer Research C, Lundgren S, Borresen-Dale AL, Kristensen V, Warnberg F, Hallett M, et al. Molecular features of subtype-specific progression from ductal carcinoma in situ to invasive breast cancer. *Cell reports*. 2016;16(4):1166–79.
24. Waters AM, Ozkan-Dagliyan I, Vaseva AV, Fer N, Strathern LA, Hobbs GA, Tessier-Cloutier B, Gillette WK, Bagni R, Whiteley GR, et al. Evaluation of the selectivity and sensitivity of isoform- and mutation-specific RAS antibodies. *Sci Signal*. 2017;10(498):eaao3332.
25. Smid M, Wang Y, Zhang Y, Sieuwerts AM, Yu J, Klijn JG, Foekens JA, Martens JW. Subtypes of breast cancer show preferential site of relapse. *Cancer Res*. 2008;68(9):3108–14.
26. Perou CM, Sorlie T, Eisen MB, van de Rijn M, Jeffrey SS, Rees CA, Pollack JR, Ross DT, Johnsen H, Akslen LA, et al. Molecular portraits of human breast tumours. *Nature*. 2000;406(6797):747–52.
27. Knudsen ES, Ertel A, Davicioni E, Kline J, Schwartz GF, Witkiewicz AK. Progression of ductal carcinoma in situ to invasive breast cancer is associated with gene expression programs of EMT and myoepithelia. *Breast Cancer Res Treat*. 2012;133(3):1009–24.
28. Abba MC, Gong T, Lu Y, Lee J, Zhong Y, Lacunza E, Butti M, Takata Y, Gaddis S, Shen J, et al. A molecular portrait of high-grade ductal carcinoma in situ. *Cancer Res*. 2015;75(18):3980–90.
29. Rody A, Karn T, Liedtke C, Pusztai L, Ruckhaeberle E, Hankaer L, Gaetje R, Solbach C, Ahr A, Metzler D, et al. A clinically relevant gene signature in triple negative and basal-like breast cancer. *Breast Cancer Res BCR*. 2011;13(5):R97.
30. Shah SP, Roth A, Goya R, Oloumi A, Ha G, Zhao Y, Turashvili G, Ding J, Tse K, Haffari G, et al. The clonal and mutational evolution spectrum of primary triple-negative breast cancers. *Nature*. 2012;486(7403):395–9.
31. Bargonetti J, Prives C. Gain-of-function mutant p53: history and speculation. *J Mol Cell Biol*. 2019;11(7):605–9.
32. Jedezsko C, Victor BC, Podgorski I, Sloane BF. Fibroblast hepatocyte growth factor promotes invasion of human mammary ductal carcinoma in situ. *Can Res*. 2009;69(23):9148–55.
33. Huper G, Marks JR. Isogenic normal basal and luminal mammary epithelial isolated by a novel method show a differential response to ionizing radiation. *Cancer Res*. 2007;67(7):2990–3001.
34. Smart CE, Morrison BJ, Saunus JM, Vargas AC, Keith P, Reid L, Wockner L, Askarian-Amiri M, Sarkar D, Simpson PT, et al. In vitro analysis of breast cancer cell line tumourspheres and primary human breast epithelia mammospheres demonstrates inter- and intrasphere heterogeneity. *PLoS One*. 2013;8(6):e64388.
35. Dong Q, Wang D, Bandyopadhyay A, Gao H, Gorena KM, Hildreth K, Rebel VI, Walter CA, Huang C, Sun LZ. Mammospheres from murine mammary stem cell-enriched basal cells: clonal characteristics and repopulating potential. *Stem Cell Res*. 2013;10(3):396–404.
36. Ringberg A, Anagnostaki L, Anderson H, Idvall I, Ferno M. South Sweden breast cancer G: Cell biological factors in ductal carcinoma in situ (DCIS) of the breast-relationship to ipsilateral local recurrence and histopathological characteristics. *Eur J Cancer*. 2001;37(12):1514–22.
37. Molinaro AM, Sison JD, Ljung BM, Tlsty TD, Kerlikowske K. Risk prediction for local versus regional/metastatic tumors after initial ductal carcinoma in situ diagnosis treated by lumpectomy. *Breast Cancer Res Treat*. 2016;157(2):351–61.
38. Bergholtz H, Lien TG, Swanson DM, Frigessi A. Oslo breast cancer research C, daidone MG, tost J, warnberg F, sorlie T: contrasting DCIS and invasive breast cancer by subtype suggests basal-like DCIS as distinct lesions. *NPJ Breast Cancer*. 2020;6:26.
39. Zheng ZY, Li J, Li F, Zhu Y, Cui K, Wong ST, Chang EC, Liao YH. Induction of N-Ras degradation by flunarizine-mediated autophagy. *Sci Rep*. 2018;8(1):16932.
40. Goldstein LJ, Mansutti M, Levy C, Chang JC, Henry S, Fernandez-Perez I, Prausova J, Staroslawska E, Viale G, Butler B, et al. A randomized, placebo-controlled phase 2 study of paclitaxel in combination with reparixin compared to paclitaxel alone as front-line therapy for metastatic triple-negative breast cancer (FRida). *Breast Cancer Res Treat*. 2021;190(2):265–75.
41. Krug K, Mertins P, Zhang B, Hornbeck P, Raju R, Ahmad R, Szucs M, Mundt F, Forestier D, Jane-Valbuena J, et al. A curated resource for phosphosite-specific signature analysis. *Mol Cell Proteomics*. 2019;18(3):576–93.

Publisher's Note

Springer Nature remains neutral with regard to jurisdictional claims in published maps and institutional affiliations.